Linear optical controlled-NOT gate in the coincidence basis

T. C. Ralph,* N. K. Langford, T. B. Bell, and A. G. White
Centre for Quantum Computer Technology, Department of Physics, University of Queensland, Queensland 4072, Australia
(Received 16 December 2001; published 20 June 2002)

We describe the operation and tolerances of a nondeterministic, coincidence basis, quantum controlled-NOT gate for photonic qubits. It is constructed solely from linear optical elements and requires only a two-photon source for its demonstration. Its success probability is 1/9.

DOI: 10.1103/PhysRevA.65.062324 PACS number(s): 03.67.−a

I. INTRODUCTION

Qubits based on the polarization state of individual photons have the advantage of low decoherence rates and are easily manipulated at the single qubit level. Optical parametric amplification experiments have been very successful in producing and analyzing a large range of two-photon entangled states [1–4]. A key ''trick'' in these types of experiments is to work in the coincidence basis in which only events where two photons are detected in the same, narrow time window are recorded. The entangled state postselected this way may be a pure Bell state even though the total state is nondeterministic and may have experienced considerable mixing from photon loss. Such systems are not scalable in the quantum computational sense in their present form but nonetheless provide an excellent testing ground for quantum information concepts. Useful application of this type of technology seems much closer in the realm of quantum communications.

A key two qubit gate is the controlled-NOT (CNOT) gate. A deterministic controlled-NOT gate would require either very high nonlinearities [5] or very complex linear networks [6]. Building on the latter ideas a linear, coincidence basis CNOT has been described [7] which could be a useful test-bed. However it requires a four-photon input, which is challenging. Two photon coincidence basis gates, which perform some, but not all, of the operations of a controlled-NOT gate have also been described [8–10].

In this paper we discuss a linear, coincidence basis gate which performs all the operations of a controlled-NOT gate and requires only a two-photon input [11]. In Sec. II we describe its construction and ideal operation. In Sec. III we consider the effect of imperfections in its construction, particularly focusing on the effect of beam splitter and mode-matching errors on the gate's efficacy as a Bell state analyzer. In Sec. IV we conclude. Recently Hofmann and Takeuchi have independently described a very similar gate [12]. Our analysis should also apply to their construction.

II. THE GATE

The gate is shown in Fig. 1. All beam splitters, $B1$, $B2$, $B3$, $B4$, and $B5$ are assumed asymmetric in phase. That is, it is assumed that the operator input-output relations (the Heisenberg equations) between the two input mode operators (a_{in} and b_{in}) and the corresponding output operators (a_{out} and b_{out}) for the beam splitters have the general form

$$a_{out}=\sqrt{\eta}a_{in}+\sqrt{1-\eta}b_{in},$$
$$b_{out}=\sqrt{1-\eta}a_{in}-\sqrt{\eta}b_{in}, \tag{1}$$

where η $(1-\eta)$ is the reflectivity (transmittivity) of the beam splitter. Reflection off the bottom produces the sign change except for $B1$ and $B2$ which have a sign change by reflection off the top. This phase convention simplifies the algebra but other phase relationships will work equally well in practice. Beam splitters $B3$ and $B4$ are both 50:50 ($\eta=1/2$). The beam splitters $B1$, $B2$, and $B5$ have equal reflectivities of one-third ($\eta=1/3$).

We employ dual rail logic such that the ''control in'' qubit is represented by the two bosonic mode operators c_H and c_V. A single photon occupation of c_H with c_V in a vacuum state will be our logical 0, which we will write $|H\rangle_c$ (to avoid confusion with the vacuum state); while a single photon occupation of c_V with c_H in a vacuum state will be our logical 1, which we will write $|V\rangle_c$. Superposition states can also be formed via beam splitter interactions. Similarly the ''target in'' is represented by the bosonic mode operators t_H and t_V and the states $|H\rangle_t$ and $|V\rangle_t$, with the same interpretations as for the control. The use of H and V to describe the states of the qubits of course alludes to the usual encoding in polarization [13]. To go from polarization encoding to dual rail

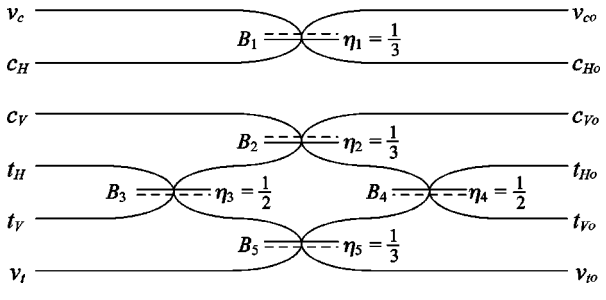

FIG. 1. Schematic of the coincidence controlled-NOT gate. Dashed line indicates the surface from which a sign change occurs upon reflection. The control modes are c_H and c_V. The target modes are t_H and t_V. The modes v_c and v_t are unoccupied ancillary modes.

*Email address: ralph@physics.uq.edu.au

spatial encoding and vice versa in the lab requires a polarizing beam splitter and half-wave plate.

The Heisenberg equations relating the control (c_H, c_V) and target (t_H, t_V) input modes to their corresponding outputs are

$$c_{H_O} = \frac{1}{\sqrt{3}}(\sqrt{2}v_c + c_H),$$

$$c_{V_O} = \frac{1}{\sqrt{3}}(-c_V + t_H + t_V),$$

$$t_{H_O} = \frac{1}{\sqrt{3}}(c_V + t_H + v_t),$$

$$t_{V_O} = \frac{1}{\sqrt{3}}(c_V + t_V - v_t),$$

$$v_{c_O} = \frac{1}{\sqrt{3}}(-v_c + \sqrt{2}c_H),$$

$$v_{t_O} = \frac{1}{\sqrt{3}}(t_H - t_V - v_t). \tag{2}$$

Ancillary vacuum input modes v_c and v_t complete the network. The gate operates by causing a sign shift in the interferometer formed by the splitting and remixing of the target modes, conditional on the presence of a photon in the c_V mode. Thus the target modes swap if the control is in the state $|V\rangle_c$ but do not if the control is in state $|H\rangle_c$. This is always true when a coincidence is measured between the control and target outputs (photons are detected at the same time). However, such coincidences occur only one-ninth of the time, on average. The other eight times out of nine either the target or the control or both do not contain a photon. This can be seen explicitly by calculating the output state of the system in the Schrödinger picture. Consider the general input state

$$\begin{aligned}|\phi\rangle &= (\alpha|HH\rangle + \beta|HV\rangle + \gamma|VH\rangle + \delta|VV\rangle)|00\rangle \\ &= (\alpha c_H^\dagger t_H^\dagger + \beta c_H^\dagger t_V^\dagger + \gamma c_V^\dagger t_H^\dagger \\ &\quad + \delta c_V^\dagger t_V^\dagger)|0000\rangle|00\rangle \end{aligned} \tag{3}$$

where the ordering in the kets is $|n_{cH}n_{cV}n_{tH}n_{tV}\rangle|n_{vc}n_{vt}\rangle$ with $n_{cH} = c_H^\dagger c_H$, etc., and we use the shorthand $|1010\rangle = |HH\rangle$, etc., where appropriate. For a time symmetric linear network such as that in Fig. 1, the output state can be directly obtained from the input state, Eq. (3), by substituting input operators for the output operators given by Eq. (2). Thus we obtain

$$\begin{aligned}|\phi\rangle_{out} &= (\alpha c_{H_O}^\dagger t_{H_O}^\dagger + \beta c_{H_O}^\dagger t_{V_O}^\dagger + \gamma c_{V_O}^\dagger t_{H_O}^\dagger + \delta c_{V_O}^\dagger t_{V_O}^\dagger)|0000\rangle|00\rangle \\ &= \frac{1}{3}\{\alpha|HH\rangle + \beta|HV\rangle + \gamma|VV\rangle + \delta|VH\rangle + \sqrt{2}(\alpha+\beta)|0100\rangle|10\rangle + \sqrt{2}(\alpha-\beta)|0000\rangle|11\rangle + (\alpha+\beta)|1100\rangle|00\rangle \\ &\quad + (\alpha-\beta)|1000\rangle|01\rangle + \sqrt{2}\alpha|0010\rangle|10\rangle + \sqrt{2}\beta|0001\rangle|10\rangle - \sqrt{2}(\gamma+\delta)|0200\rangle|00\rangle - (\gamma-\delta)|0100\rangle|01\rangle \\ &\quad + \sqrt{2}\gamma|0020\rangle|00\rangle + (\gamma-\delta)|0010\rangle|01\rangle + (\gamma+\delta)|0011\rangle|00\rangle + (\gamma-\delta)|0001\rangle|01\rangle + \sqrt{2}\delta|0002\rangle|00\rangle\} \end{aligned} \tag{4}$$

The state postselected in the coincidence basis is then just

$$|\phi\rangle_{cb} = \alpha|HH\rangle + \beta|HV\rangle + \gamma|VV\rangle + \delta|VH\rangle, \tag{5}$$

occurring with probability one-ninth. The relationship between Eq. (3) and Eq. (5) is a controlled-NOT transformation.

It is also useful to look at the coincidence number expectation values, obtained directly from the Heisenberg equations [Eq. (2)]. These can be interpreted as the predicted output coincident count rates normalized to the input pair rate. An example is given in Table I which shows the count rates for logical basis inputs. A more interesting case is to use the four Bell states

TABLE I. Coincident expectation values calculated for the four logical basis inputs.

Input	$\langle n_{cH_O}n_{tH_O}\rangle$	$\langle n_{cH_O}n_{tV_O}\rangle$	$\langle n_{cV_O}n_{tH_O}\rangle$	$\langle n_{cV_O}n_{tV_O}\rangle$
$\|H\rangle_c\|H\rangle_t$	1/9	0	0	0
$\|H\rangle_c\|V\rangle_t$	0	1/9	0	0
$\|V\rangle_c\|H\rangle_t$	0	0	0	1/9
$\|V\rangle_c\|V\rangle_t$	0	0	1/9	0

$$|\psi^\pm\rangle = \frac{1}{\sqrt{2}}(|H\rangle_c|H\rangle_t \pm |V\rangle_c|V\rangle_t),$$

$$|\phi^\pm\rangle = \frac{1}{\sqrt{2}}(|H\rangle_c|V\rangle_t \pm |V\rangle_c|H\rangle_t) \tag{6}$$

TABLE II. Coincident expectation values calculated in the superposition basis for the four Bell states.

Input	$\langle n_{cS_1} n_{tH_O}\rangle$	$\langle n_{cS_2} n_{tV_O}\rangle$	$\langle n_{cS_1} n_{tH_O}\rangle$	$\langle n_{cS_2} n_{tV_O}\rangle$
$\lvert\psi^+\rangle$	1/9	0	0	0
$\lvert\psi^-\rangle$	0	1/9	0	0
$\lvert\phi^+\rangle$	0	0	1/9	0
$\lvert\phi^-\rangle$	0	0	0	1/9

as inputs and to detect the control in the superposition basis by mixing the control outputs on a 50:50 beam splitter before detection:

$$c_{S_1} = \frac{1}{\sqrt{2}}(c_{H_O} + c_{V_O}),$$
$$c_{S_2} = \frac{1}{\sqrt{2}}(c_{H_O} - c_{V_O}). \tag{7}$$

In Table II the count rates for this arrangement are presented, showing the ability to distinguish all four Bell states (albeit with nonunit efficiency). Such a Bell state analyzer could have significant applications in quantum communications. In the next section we will use this application as an example in order to investigate the effect of nonoptimal parameters on the gate.

III. NONOPTIMAL OPERATION

The accuracy with which the gate operates will be determined by how closely the parameters of the constructed gate correspond to those of the idealized gate of the previous section. We can identify three potential sources of error: incorrect beam splitter ratios; nonunit mode matching, and timing errors. One advantage of working in the coincidence basis is that losses and detector inefficiency can be ignored because they take the system out of the coincidence basis and thus their only effect is to reduce the count rate.

Timing errors. Correct gate operation depends on indistinguishability of the paths taken by the two photons through the network. This means that they must arrive simultaneously at the central beam splitter to an accuracy of a fraction of their coherence length. Photon coherence length in down-conversion experiments is generally determined by predetection frequency filtering and can be of order 100 wavelengths. Locking path lengths on this scale should not be a major problem.

Beam splitter ratios. The effect of nonoptimal beam splitter ratios can be investigated by deriving the operator equations [Eq. (2)] more generally, with arbitrary beam splitter ratios. For simplicity we assume that the beam splitters all came from the same ''production run'' such that any deviation from the optimal value is common. That is, we might suppose that both the 50:50 beam splitters actually have a reflectivity of η' while the three 33:67 beam splitters all actually have reflectivities η. The Heisenberg equations are then

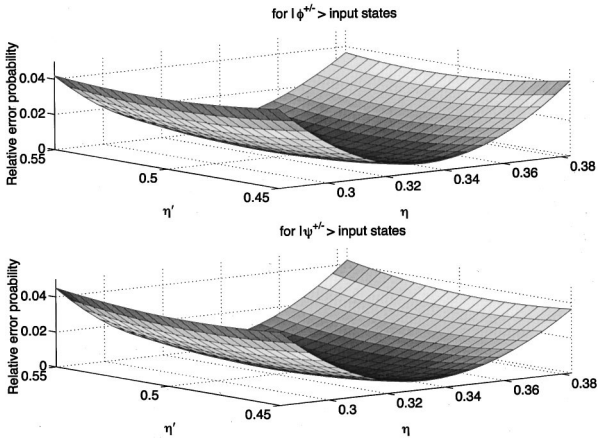

FIG. 2. Relative error probabilities, i.e., error rate/total rate, for Bell state analysis as a function of beam splitter ratios close to the optimum values of $\eta' = 1/2$ and $\eta = 1/3$.

$$c_{H_O} = \sqrt{\eta} c_H + \sqrt{1-\eta} v_c,$$
$$c_{V_O} = -\sqrt{\eta} c_V + \sqrt{(1-\eta)\eta'} t_H + \sqrt{(1-\eta)(1-\eta')} t_V,$$
$$t_{H_O} = \sqrt{\eta} t_H + \sqrt{(1-\eta)\eta'} c_V + \sqrt{(1-\eta)(1-\eta')} v_t$$
$$t_{V_O} = \sqrt{\eta}) t_V + \sqrt{(1-\eta)(1-\eta')} c_V - \sqrt{(1-\eta)\eta'} v_t,$$
$$v_{c_O} = -\sqrt{\eta} v_c + \sqrt{1-\eta} c_H,$$
$$v_{t_O} = \sqrt{(1-\eta)(1-\eta')} t_H - \sqrt{(1-\eta)\eta'} t_V - \sqrt{\eta} v_t. \tag{8}$$

In general, the effect of varying the beam splitter ratios is input state dependent. However, for small deviations from the optimum values Bell state analysis is approximately state independent and serves as a useful diagnostic [14]. In Fig. 2 we plot the error probability in distinguishing the Bell states as a function of η and η' in the region close to their optimum values. The dependence of the error probability on η' is mirror imaged between the $\lvert\psi^\pm\rangle$ and the $\lvert\phi^\pm\rangle$ Bell states.

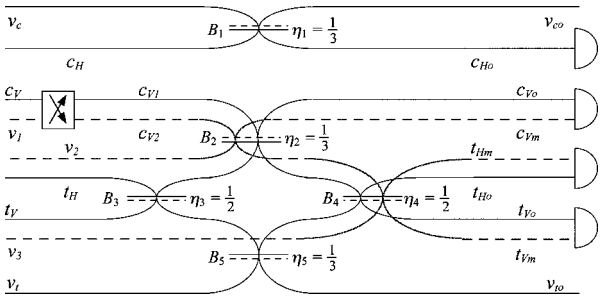

FIG. 3. Schematic diagram of the coincidence controlled-NOT gate including the effects of mode matching. The mismatch is represented by splitting c_V into two orthogonal modes c_{V1} and c_{V2}. Ancillary modes v_1, v_2, and v_3 interact with the propagating mismatch.

TABLE III. As for Table I, now allowing for mode matching ξ. (For perfect mode match, $\xi=1$; for complete mode mismatch $\xi=0$.)

Input	$\langle n_{cH_D} n_{tH_D}\rangle$	$\langle n_{cH_D} n_{tV_D}\rangle$	$\langle n_{cV_D} n_{tH_D}\rangle$	$\langle n_{cV_D} n_{tV_D}\rangle$
$\|H\rangle_c\|H\rangle_t$	1/9	0	0	0
$\|H\rangle_c\|V\rangle_t$	0	1/9	0	0
$\|V\rangle_c\|H\rangle_t$	0	0	$(2/9)(1-\xi)$	1/9
$\|V\rangle_c\|V\rangle_t$	0	0	1/9	$(2/9)(1-\xi)$

However, this dependence is negligible in the region close to $\eta'=1/2$. The dependence on η is more pronounced. For an η of $1/3\pm0.01$ (and η' of $1/2\pm0.05$) error rates of about 0.7% are predicted. Such uncertainties are standard with current beam splitter technology, and we conclude that errors below 1.0% are realistic.

Mode matching errors. Mode matching in nonclassical interference experiments is generally quite difficult and may be identified as a major contributor to nonunit visibility. Given the key role of nonclassical interference in the controlled-NOT gate we may expect mode matching errors to be of some significance.

In order to model the mismatch of input modes at the central beam splitter, ancillary modes v_1, v_2, and v_3 (originally in the vacuum state) are introduced to interact with the propagating mismatch mode. The additional output modes are labeled c_{V_m}, c_{H_m}, and t_{V_m} (see Fig. 3). The mode c_v is assumed to be the source of the mismatch, after having passed through some kind of optical element that has misaligned it:

$$c_{V_1}=\sqrt{\xi}c_V+\sqrt{1-\xi}v_1,$$

$$c_{V_2}=-\sqrt{1-\xi}c_V+\sqrt{\xi}v_1.$$

The parameter ξ quantifies the degree of mode matching between the control and target modes at the central beam splitter. So long as the modes are matched reasonably well, c_{V_1} can be considered a sort of ''primary'' mode. It interacts with the output from beam splitter B_3 in the same way as for the case neglecting mode matching. The mismatch component c_{V_2} interacts only with the newly introduced vacuum modes.

The equations for the output modes of the quantum controlled-NOT gate, including the effects of a mode mismatch, are

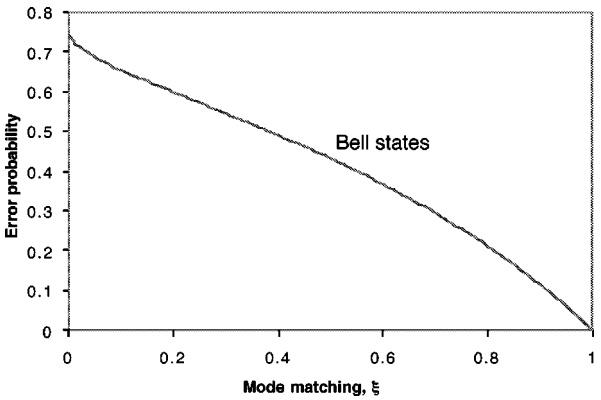

FIG. 4. Error probability as a function of mode matching for the four Bell states.

$$v_{c_O}=\frac{1}{\sqrt{3}}(-v_c+\sqrt{2}c_H),$$

$$c_{H_O}=\frac{1}{\sqrt{3}}(\sqrt{2}v_c+c_H),$$

$$c_{V_O}=\frac{1}{\sqrt{3}}(-\sqrt{\xi}c_V-\sqrt{1-\xi}v_1+t_H+t_V),$$

$$c_{V_m}=\frac{1}{\sqrt{3}}(\sqrt{1-\xi}c_V-\sqrt{\xi}v_1+\sqrt{2}v_2),$$

$$t_{H_O}=\frac{1}{\sqrt{3}}(\sqrt{\xi}c_V+t_H+\sqrt{1-\xi}v_1+v_t), \tag{9}$$

$$t_{H_m}=\frac{1}{\sqrt{3}}\left(-\sqrt{1-\xi}c_V+\sqrt{\xi}v_1+\frac{1}{\sqrt{2}}v_2+\sqrt{\frac{3}{2}}v_3\right),$$

$$t_{V_O}=\frac{1}{\sqrt{3}}(\sqrt{\xi}c_V+t_V+\sqrt{1-\xi}v_1-v_t),$$

$$t_{V_m}=\frac{1}{\sqrt{3}}\left(-\sqrt{1-\xi}c_V+\sqrt{\xi}v_1+\frac{1}{\sqrt{2}}v_2-\sqrt{\frac{3}{2}}v_3\right),$$

$$v_{t_O}=\frac{1}{\sqrt{3}}(t_H-t_V-v_t).$$

Now, when measuring the coincidences, the detectors see a combination of the counts from both the primary modes and

TABLE IV. As for Table II, now allowing for mode match ξ.

Input	$\langle n_{cS_1} n_{tH_D}\rangle$	$\langle n_{cS_2} n_{tH_D}\rangle$	$\langle n_{cS_1} n_{tV_D}\rangle$	$\langle n_{cS_2} n_{tV_D}\rangle$
$\|\psi^+\rangle$	$(1/18)(1+\sqrt{\xi})$	$(1/18)(1-\sqrt{\xi})$	$(1/18)(1-\xi)$	$(1/18)(1-\xi)$
$\|\psi^-\rangle$	$(1/18)(1-\sqrt{\xi})$	$(1/18)(1+\sqrt{\xi})$	$(1/18)(1-\xi)$	$(1/18)(1-\xi)$
$\|\phi^+\rangle$	$(1/18)(1-\xi)$	$(1/18)(1-\xi)$	$(1/18)(1+\sqrt{\xi})$	$(1/18)(1-\sqrt{\xi})$
$\|\phi^-\rangle$	$(1/18)(1-\xi)$	$(1/18)(1-\xi)$	$(1/18)(1-\sqrt{\xi})$	$(1/18)(1+\sqrt{\xi})$

the mismatch modes (see Fig. 3). For example, when detecting coincidences of horizontally polarized photons, the count rate becomes

$$\begin{aligned}\langle n_{cH_D} n_{tH_D}\rangle &= \langle n_{cH_O}(n_{tH_O}+n_{tH_m})\rangle \\ &= \langle n_{cH_O} n_{tH_O}\rangle + \langle n_{cH_O} n_{tH_m}\rangle\end{aligned}$$

and similarly,

$$\begin{aligned}\langle n_{cH_D} n_{tV_D}\rangle &= \langle n_{cH_O} n_{tV_O}\rangle + \langle n_{cH_O} n_{tV_m}\rangle, \\ \langle n_{cV_D} n_{tH_D}\rangle &= \langle n_{cV_O} n_{tH_O}\rangle + \langle n_{cV_O} n_{tH_m}\rangle \\ &\quad + \langle n_{cV_m} n_{tH_O}\rangle + \langle n_{cV_m} n_{tH_m}\rangle, \\ \langle n_{cV_D} n_{tV_D}\rangle &= \langle n_{cV_O} n_{tV_O}\rangle + \langle n_{cV_O} n_{tV_m}\rangle \\ &\quad + \langle n_{cV_m} n_{tV_O}\rangle + \langle n_{cV_m} n_{tV_m}\rangle. \end{aligned} \tag{10}$$

These moments are summarized for logical inputs in Table III. As expected, the mode mismatch has not affected the controlled-NOT operation when the control is ''off'' (i.e., when c_H is occupied). In this case, there is no interaction at beam splitter B_2 (Fig. 3) and thus no nonclassical interference. However, when the control is ''on,'' the effects of the mismatch are noticeable.

Interestingly, the mismatch adds extra terms rather than redistributing the probabilities of the counts measured in the ideal case. Coincidence events which previously were disallowed due to the nonclassical interference can now appear as error events because of the mismatch. Thus the probabilities that are being redistributed are those for the states that were not detected in the ideal case (the states that had been postselected out).

We now consider the performance of the gate as a Bell state analyzer in the presence of mode mismatch. As in the ideal case, another beam splitter is added to the outputs of the control qubit. Another ancillary mode v_4 must be added to interact with the mismatch mode c_{V_m}.

The beam splitter outputs are given in the Heisenberg picture by

$$\begin{aligned} c_{S_{1O}} &= \frac{1}{\sqrt{2}}(c_{H_O}+c_{V_O}), \\ c_{S_{1M}} &= \frac{1}{\sqrt{2}}(v_4+c_{V_m}), \\ c_{S_{2O}} &= \frac{1}{\sqrt{2}}(c_{H_O}-c_{V_O}), \\ c_{S_{2M}} &= \frac{1}{\sqrt{2}}(v_4-c_{V_m}). \end{aligned} \tag{11}$$

Each detector receives counts from both of the modes incident on it, so the expectation values must be combined in a similar way to Eq. (10). The coincidence count rates are given in Table IV. Using $\xi=1$ yields the perfectly matched case calculated previously (see Table II). The error probability for Bell state discrimination is plotted in Fig. 4. For small mismatch the error is approximately equal to the percentage mismatch. Clearly, good Bell state discrimination will require accurate mode matching to the central beam splitter.

IV. CONCLUSION

We have described a nondeterministic quantum controlled-NOT gate that operates with one-ninth efficiency, constructed solely from linear optical elements. We have investigated the behavior of the gate with variation in both the beam splitter and mode match values and conclude that a demonstration is feasible with current optical technology. Aside from its value as a test bed system, such a gate could be made scalable if photon-number QND detectors were added to each output. This latter system would also act as an efficient Bell state analyzer, which is an important component in some quantum algorithms, notably quantum teleportation.

[1] P. G. Kwiat, K. Mattle, H. Weinfurter, A. Zeilinger, A. V. Sergienko, and Y. Shih, Phys. Rev. Lett. **75**, 4337 (1995).

[2] J. Brendel, N. Gisin, W. Tittel, and H. Zbinden, Phys. Rev. Lett. **82**, 2594 (1999).

[3] A. G. White, D. F. V. James, P. H. Eberhard, and P. G. Kwiat, Phys. Rev. Lett. **83**, 3103 (1999).

[4] A. G. White, D. F. V. James, W. J. Munro, and P. G. Kwiat, Phys. Rev. A **65**, 012301 (2001).

[5] G. J. Milburn, Phys. Rev. Lett. **62**, 2124 (1988).

[6] E. Knill, R. Laflamme, and G. Milburn, Nature (London) **409**, 46 (2001).

[7] T. C. Ralph, A. G. White, W. J. Munro, and G. J. Milburn, Phys. Rev. A **65**, 012314 (2001).

[8] D. Bouwmeester, J. W. Pan, K. Mattle, M. Eibl, H. Weinfurter, and A. Zeilinger, Nature (London) **390**, 575 (1997).

[9] J. W. Pan, C. Simon, C. Brukner, and A. Zeilinger, Nature (London) **410**, 1067 (2001).

[10] T. B. Pittman, B. C. Jacobs, J. D. Franson, e-print quant-ph/0109128 (unpublished).

[11] T. C. Ralph, provisional patent, (August 2001).

[12] H. F. Hofmann and S. Takeuchi, e-print quant-ph/0111092 (unpublished).

[13] Of course, other degrees of freedom, such as orbital angular momentum, could be used in place of polarization.

[14] Full characterization of the gate via quantum process tomography is currently under investigation.